Switching formation control of multi-lane autonomous vehicle platoons robust to relative position measurement noises

Bastiaan G. L. Meere * **Baris Fidan** **
W. P. Maurice H. Heemels *

* *Department of Mechanical Engineering, Eindhoven University of Technology, The Netherlands (e-mail: basmeere@gmail.com, w.p.m.h.heemels@tue.nl).*
** *Department of Mechanical and Mechatronics Engineering, University of Waterloo, Waterloo ON, Canada (e-mail: fidan@uwaterloo.ca)*

Abstract: This paper studies formation control of multi-lane platoons of vehicles, endowed with local positioning capabilities, under the influence of noises and inconsistencies of inter-vehicle relative position measurements. We propose a distributed two-level control framework that consists of a high-level relative position based distributed formation control scheme and low-level individual dynamic controllers of the platoon vehicles. The proposed formation control scheme utilizes deadzone based switching for robustness against sensor noises and adaptive longitudinal controllers for enabling the platoon of heterogeneous vehicles to track the desired platoon velocity.

Keywords: Cooperative navigation, multi-vehicle systems, multi-agent systems

1. INTRODUCTION

To address the significant increase in traffic congestion, accident, and environmental pollution issues in recent decades linked to an increase of vehicles on the road (Smith (2016)), the study of cooperative control of connected autonomous/automated vehicles (CAVs) has grown enormously. It has become a large interdisciplinary research topic with the potential to significantly improve traffic flow and safety, reduce pollutant emissions, and enhance driving comfort (Chan et al. (2012)). One particular CAV approach to address the aforementioned issues is to have vehicles operate at small inter-vehicle distances in a spatially coordinated scheme often referred to as a platoon. In this paper, we consider a vehicle platoon as in De La Fortelle et al. (2014), that is composed of three or more vehicles maintaining a single or multi-lane formation and that has neither a leading vehicle nor a centralized controller/supervisor.

Many of the recent studies on vehicle formation control, including Guanetti et al. (2018) and Li et al. (2017b), focus on acquiring and maintaining desired inter-vehicle distances using reactive spacing control methods. Some of these recent studies also utilize advanced robust and optimal control methods, such as $\mathcal{H}_\infty$ control (Li et al. (2017a)), model predictive control (Dolk et al. (2017)) and sliding mode control (Li et al. (2018)). The aforementioned papers (Guanetti et al. (2018); Li et al. (2017b,a); Dolk et al. (2017); Li et al. (2018)), however, only consider vehicle platoons on a single straight lane. One of the first works introducing the multi-lane formation control concept is Kato et al. (2002), where it is shown that safety levels increase as vehicles are able to coordinate and cooperate with vehicles in both the same lane and neighbouring ones. Since then, a variety of studies have looked into formation and reconfiguration (Firoozi et al. (2021)) and target assignment (Cai et al. (2019)). Most of these works implement some form of a bi-level motion control framework. The upper level is the planning layer responsible for geometric structure generation and formation control. The lower level consists of individual dynamic controllers for each vehicle.

In Oh et al. (2015), the formation control of multi-agent systems is categorized into position, displacement, and distance based control according to the utilized types of sensed and controlled variables. In displacement based control, where each agent measures the relative positions of others with respect to its own coordinate system, the desired formation is specified by the relative positions between vehicles. The formation, therefore, does not require each agent to know its absolute position with respect to a global coordinate system as is the case in position based control. Furthermore, by using relative positions as opposed to inter-vehicle distances, the interaction graph is not required to acquire and maintain rigidity or persistence. This suits a platooning application as it is not limited in its formation shapes and can dynamically accommodate joining and leaving vehicles. These reasons motivate us to consider displacement (relative position) based control for the formation control scheme.

Despite the considerable amount of research on the control of multi-lane platoons, the literature on the effects of sensor noise is limited. In contrast, these effects have been studied for some general interconnected system consensus problems, assuming the noise to have an upper magnitude

bound (Sancar et al. (2015)) or some stochastic approximation (Huang and Manton (2009)). In this paper, we consider magnitude-bounded noise on the relative position measurements of neighbouring vehicles to match the framework introduced in Hendrickx et al. (2019).

Without properly addressing them, sensor noises have been shown to lead to distorted formations and unexpected and undesirable movements (De Marina et al. (2014)). Aiming to fill this gap, the contribution of this work is the design of a distributed control scheme for multi-lane platoons of heterogeneous vehicles in the presence of sensor noise. The control framework is inspired by the bi-level control hierarchy of Zheng et al. (2021), however, instead of the distance based formation control algorithm, we apply a relative position based strategy with the threshold function from Hendrickx et al. (2019) to make it robust to sensor noise. Compared with the works of, (Sancar et al. (2015); Hendrickx et al. (2019)), we extend the application of this threshold function from 1-dimensional single-lane platoons to 2-dimensional multi-lane configurations. Furthermore, we implement a longitudinal adaptive controller and a lane-keeping lateral controller. To make the platoon adapt to the shape of the road we utilize a Frenet coordinate system as in Navarro et al. (2016). The strengths of the proposed framework and distributed control scheme are demonstrated through numerical simulations.

The paper is organized as follows: The problem statement is presented in Section 2 and the necessary background is provided in Section 3. Section 4 details the controller design after which Section 5 shows the simulation results. The conclusions are provided in Section 6.

2. PROBLEM STATEMENT

Consider a platoon of N vehicles distributed over several lanes of a highway as shown in Figure 1. The dotted lines represent the sensing and communication links among the N vehicles. Assume that each agent can determine its position within a lane, e.g. using video, laser, and/or infrared systems as in Cudrano et al. (2020) and the relative position of neighbouring agents using LIDAR, radar, and/or cameras (Yeong et al. (2021)) all with respect to its own coordinate frame. Assume also that by using vehicle-to-vehicle (V2V) communication, the agents can exchange their own lane position estimates, which are generally more accurate than the estimates by other vehicles, among neighbours.

The goal of this work is to design a distributed control scheme for such a vehicle platoon with three objectives in mind. First of all, the vehicles should drive in the centre of their lane. Secondly, the platoon moves at a certain group velocity and, thirdly, the platoon should maintain a desired geometric formation. These three objectives can be conflicting at times and the presence of noise can introduce uncertainty. Therefore, we strive for control solutions that lead to performance within certain bounds, e.g., by allowing some elasticity in the formation, instead of achieving rigidity.

In the following sections, we detail the design of a hierarchical platoon control architecture composed of a distributed formation control layer and individual vehicle

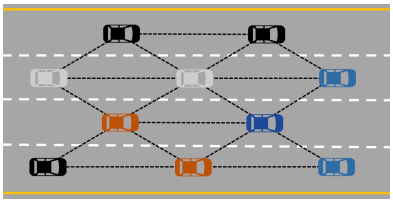

Fig. 1. A multi-lane heterogeneous vehicle platoon

dynamic controllers. The control design task can then be summarized as finding appropriate longitudinal, lateral and formation control algorithms, which guarantee the stability of the overall system and aim to achieve the three control objectives within specific bounds.

3. BACKGROUND & ARCHITECTURAL SETUP

We consider a vehicle formation in $\mathbb{R}^2$, consisting of $N \geq 2$ vehicles labeled by $1, \ldots, N$, whose neighbor relationships are described by an undirected graph G with the vertex set $\mathcal{V} = \{1, \ldots, N\}$ and the edge set $\mathcal{E} \subseteq \mathcal{V} \times \mathcal{V}$. We assume that there is no self-edge, i.e., $(i, i) \notin \mathcal{E}$ for any $i \in \mathcal{V}$. The set of neighbors of $i \in \mathcal{V}$ is denoted by $\mathcal{N}_i := \{j \in \mathcal{V} : (i, j) \in \mathcal{E}\}$. The degree $deg(i)$ of vehicle i is the size $|\mathcal{N}_i|$ of its neighbour set $\mathcal{N}_i$.

To enable the platoon to adapt to the road shape, we employ the Frenet coordinate system (s, l), (Navarro et al. (2016)) where the coordinate vector of vehicle i at any time $t \in \mathbb{R}_{\geq 0}$ is $p_i(t) = [s_i(t), l_i(t)]^T \in \mathbb{R}^2$, $s_i(t)$ representing the longitudinal position along the lane, i.e., the distance followed along the road from an arbitrary origin at time t and $l_i(t)$ denoting the lateral position with respect to the center of a reference lane at time t. Vehicles maintaining lanes other than the reference lane will therefore have a fixed lateral offset.

The kinematics of vehicle i are described, based on the schematics shown in Fig 2, by the bicycle model

$$\begin{aligned} \dot{s}_i(t) &= u_{i,s}(t) = v_i(t) \cos \psi_i(t) \\ \dot{l}_i(t) &= u_{i,l}(t) = v_i(t) \sin \psi_i(t) \\ \dot{\psi}_i(t) &= \frac{v_i(t)}{L_i} \tan \phi_i(t) \end{aligned} \tag{1}$$

where $u_i(t) = [u_{i,s}(t), u_{i,l}(t)]^T$ is the kinematic (velocity) input and $\psi_i(t) \in \left(-\frac{\pi}{2}, \frac{\pi}{2}\right]$, $L_i \in \mathbb{R}_{>0}$ and $v_i(t) \in \mathbb{R}$ are the yaw angle, wheelbase and speed of vehicle i at time t, respectively. $\phi_i(t) \in \mathbb{R}$ is the steering angle of the front wheels and the control input of the lateral controller.

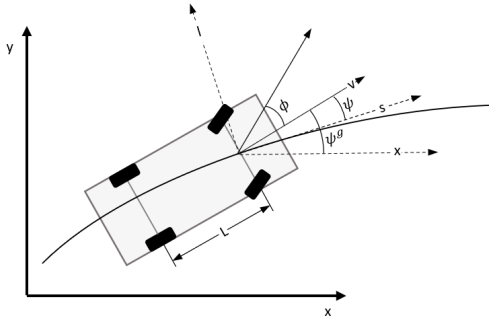

Fig. 2. The parameters of the bicycle model

The longitudinal dynamics of each vehicle $i \in \mathcal{V}$ are represented by the model (Li et al. (2017b))

$$\dot{v}_i(t) = \alpha_i T_i(t) + \beta_i v_i^2(t) + \delta_i \tag{2}$$

where $\alpha_i = \frac{\eta_{T,i}}{r_{w,i} m_i}$, $\beta_i = -\frac{C_{A,i}}{m_i}$, $\delta_i = -g f_i$ are the unknown input gain, the unknown damping coefficient and a fixed unknown disturbance, respectively. $T_i(t)$ at time $t \in \mathbb{R}_{\geq 0}$ is the input torque and control input of the longitudinal controller. The parameters $C_{A,i}$, f_i, $\eta_{T,i}$, with ranges found in Zheng et al. (2021), are the lumped aerodynamic drag coefficient, coefficient of rolling resistance and mechanical efficiency of the drive-line, respectively. m_i is the common vehicle mass as used in Buzeman et al. (1998) while g and $r_{w,i}$ are the gravity constant and wheel radius, respectively.

3.1 Formation control layer

The goal of the formation control scheme is to acquire the desired geometric vehicle formation and maintain this geometric formation when the platoon is in motion. The relative position of vehicle i with respect to each vehicle $j \in \mathcal{N}_i$ at time t is denoted by

$$d_{ij}^*(t) = p_i(t) - p_j(t) \in \mathbb{R}^2. \tag{3}$$

The measurement of (3) by vehicle i is

$$d_{ij}(t) = p_i(t) - p_j(t) + n_{ij}(t), \tag{4}$$

where $n_{ij}(t) = [n_{ij,s}(t), n_{ij,l}(t)]^T \in \mathbb{R}^2$ represents the noise in this measurement. The magnitude of n_{ij} is assumed to be bounded from above by some constant $\bar{n} > 0$, *i.e.*, $\|n_{ij,k}(t)\| \leq \bar{n}$, $k \in \{s, l\}$, for all $t \in \mathbb{R}_{\geq 0}$, where $\|.\|$ is the Euclidean norm. Since generally $n_{ij}(t) \neq n_{ji}(t)$, the vehicles have different measurements of each other's relative position.

The local formation control objective is defined as regulating

$$e_{ij}^*(t) = d_{ij}^*(t) - D_{ij}, \quad (i,j) \in \mathcal{E} \tag{5}$$

to zero, where $D_{ij} \in \mathbb{R}^2$ is the desired relative position for $(i,j) \in \mathcal{E}$. Allowing some elasticity in the formation, the relaxed practical control objective is a minimization of

$$\|d_{ij}^*(t) - D_{ij}\|, \quad (i,j) \in \mathcal{E}. \tag{6}$$

We consider the ordered desired relative positions, called the distance set, as $D := \left[\cdots D_{ij}^T \cdots\right]^T \in \mathbb{R}^{2|\mathcal{E}|}$. Clearly, not all distance sets are actually realizable in practice. Therefore, we utilize the notion of realizibility of a distance set D for a given graph G. The pair (G, D) is said to be realizable in $\mathbb{R}^2$, if there exists $p^* \in \mathbb{R}^{2N}$ such that $p_i^* - p_j^* = D_{ij}$ for all $(i,j) \in \mathcal{E}$.

Provided that (G, D) is realizable, ideal agents with single-integrator dynamics, assuming their velocity input u_i is directly applicable in (1), achieve objective (5) under the consensus control law (Ren et al. (2005))

$$u_i(t) = k_c \sum_{j \in \mathcal{N}_i} w_{ji} \left(p_j(t) - p_i(t) - D_{ji}\right), i \in \mathcal{V} \tag{7}$$

where $k_c > 0$ is a control parameter and w_{ij} are update weights, assuming there is no sensor noise, i.e. $n_{ij,x} = n_{ij,y} = 0$. In our approach below, however, we compensate for the presence of sensor noise and consider the lower-level dynamic structure, as illustrated in Fig. 3, rather than imposing single-integrator dynamics with u_i as input.

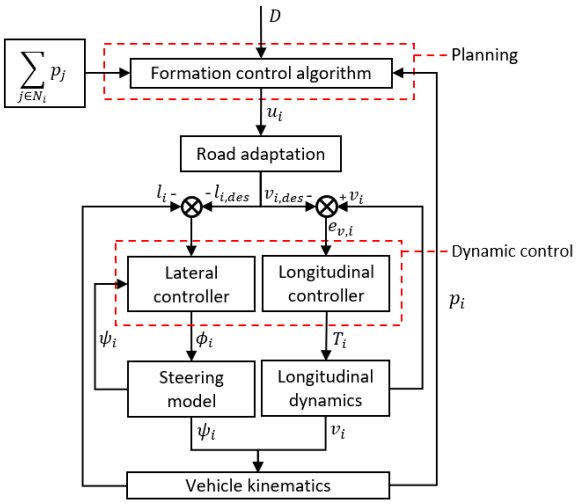

Fig. 3. Block-diagram of the proposed control design with T_i, ϕ_i and u_i as the control inputs of the longitudinal, lateral and formation controller respectively

3.2 Road adaptation

Vehicles on outer lanes travel longer distances than vehicles on inner lanes due to the larger curve radius. For vehicles in the reference lane, we translate the desired speed in the s axis ($\dot{s}_i(t)$) to a velocity command $v_{i,\text{des}}(t)$ via $\dot{s}_i(t) \simeq v_{i,\text{des}}(t)$, assuming that all vehicles are heading in the same road direction and that due to the lateral controller their headings are approximately parallel to the road. For vehicles in different lanes, we scale this translation based on the larger or smaller road curve radius.

4. CONTROLLER DESIGN

This section details the design of the individual longitudinal dynamic and lateral kinematic vehicle controllers and the distributed formation control scheme for the whole platoon, as the main components of the proposed control framework illustrated in Fig 3.

4.1 Longitudinal controller

The objective of the longitudinal controller is to generate $T_i(t)$ in (2) such that the longitudinal tracking error

$$e_{v,i}(t) = v_i(t) - v_{i,des}(t), \tag{8}$$

with $v_{i,des}(t)$ as defined in Section 3.2, is minimized. Taking the time derivative of $e_{v,i}$ along (2) yields

$$\dot{e}_{v,i}(t) = \alpha_i T_i(t) + \beta_i v_i^2(t) + \delta_i - \dot{v}_{i,\text{des}}(t). \tag{9}$$

As α_i, β_i and δ_i are unknown, we apply a modified version of the adaptive controller proposed by Zheng et al. (2021) where an additional integral term is used to reduce the steady-state error. This leads to the controller

$$\begin{aligned} T_i(t) &= \hat{\alpha}_i(t)(-k_1 e_{v,i}(t) - k_2 \omega_i(t) - \hat{\beta}_i(t) v_i^2(t) \\ &\quad - \hat{\delta}_i(t) + \dot{v}_{i,\text{des}}(t)) \\ \dot{\omega}_i(t) &= e_{v,i}(t) \end{aligned} \tag{10}$$

where $k_1, k_2 \in \mathbb{R}^+$ are the proportional and integral control gains, respectively, the variable ω_i is introduced as the integral of the velocity tracking error (8), and $\hat{\alpha}_i(t), \hat{\beta}_i(t)$ and $\hat{\delta}_i(t)$ represent the adaptive estimates of

$\bar{\alpha}_i(t) := \frac{1}{\alpha_i(t)}, \beta_i(t)$ and $\delta_i(t)$ respectively. We note that $\bar{\alpha}_i(t)$ is well-defined since $\alpha_i(t) > 0$ for all $t \in \mathbb{R}_{\geq 0}$. For further analysis, we define the parameter estimation errors

$$\begin{aligned} \tilde{\bar{\alpha}}_i(t) &= \hat{\bar{\alpha}}_i(t) - \bar{\alpha}_i \\ \tilde{\beta}_i(t) &= \hat{\beta}_i(t) - \beta_i \\ \tilde{\delta}_i(t) &= \hat{\delta}_i(t) - \delta_i \end{aligned} \tag{11}$$

for vehicle $i \in \mathcal{V}$. Substituting (10), (11) into (9) results in

$$\begin{aligned} \dot{e}_{v,i}(t) =& \frac{\hat{\bar{\alpha}}_i(t)}{\bar{\alpha}_i}(-k_1 e_{v,i}(t) - k_2\omega_i(t) - \hat{\beta}_i(t)v_i^2(t) \\ & - \hat{\delta}_i(t) + \dot{v}_{i,des}(t)) + \beta_i v_i^2(t) + \delta_i - \dot{v}_{i,\mathrm{des}}(t) \\ =& - k_1 e_{v,i}(t) - k_2\omega_i(t) - \tilde{\beta}_i(t)v_i^2(t) - \tilde{\delta}_i(t) + \frac{\tilde{\bar{\alpha}}_i(t)}{\bar{\alpha}_i}\tau_i \end{aligned} \tag{12}$$

where

$$\tau_i(t) = - k_1 e_{v,i}(t) - k_2\omega_i(t) - \hat{\beta}_i(t)v_i^2(t) - \hat{\delta}_i(t) + \dot{v}_{i,\mathrm{des}}(t) \tag{13}$$

The adaptive laws are defined as

$$\begin{aligned} \dot{\tilde{\bar{\alpha}}}_i(t) &= -\gamma_\alpha e_{v,i}(t)\tau_i(t) \\ \dot{\tilde{\beta}}_i(t) &= \gamma_\beta v_i^2(t) e_{v,i}(t) \\ \dot{\tilde{\delta}}_i(t) &= \gamma_\delta e_{v,i}(t) \end{aligned} \tag{14}$$

where $\gamma_\alpha, \gamma_\beta, \gamma_\delta > 0$ are adaptive gain constants.

Theorem 1. *Consider the nonlinear longitudinal dynamics* (2) *with unknown parameters α_i, β_i and δ_i for Vehicle i. The adaptive control law* (10)*,* (13) *and* (14) *guarantees that the vehicle speed v_i is bounded and asymptotically converges to the reference signal $v_{i,des}$.*

Proof. Consider the Lyaponuv function

$$\begin{aligned} V(t) = & \frac{1}{2}e_{v,i}^2(t) + \frac{k_2}{2}\omega_i^2(t) + \frac{1}{2\gamma_\alpha\left|\bar{\alpha}_i\right|}\tilde{\bar{\alpha}}_i^2(t) + \frac{1}{2\gamma_\beta}\tilde{\beta}_i^2(t) \\ & + \frac{1}{2\gamma_\delta}\tilde{\delta}_i^2(t), \end{aligned} \tag{15}$$

with $k_2 > 0$. The time derivative of $V(t)$ is

$$\begin{aligned} \dot{V}(t) =& e_{v,i}(t)\dot{e}_{v,i}(t) + k_2\omega_i(t)\dot{\omega}_i(t) + \frac{\tilde{\bar{\alpha}}_i(t)}{\gamma_\alpha\left|\bar{\alpha}_i\right|}\dot{\tilde{\bar{\alpha}}}_i(t) \\ & + \frac{\tilde{\beta}_i}{\gamma_\beta}(t)\dot{\tilde{\beta}}_i(t) + \frac{\tilde{\delta}_i(t)}{\gamma_\delta}\dot{\tilde{\delta}}_i(t) \end{aligned} \tag{16}$$

by substituting (12), (13) and (14) into (16) we obtain

$$\begin{aligned} \dot{V}(t) =& - k_1 e_{v,i}^2(t) + \tilde{\beta}_i(t)(\dot{\tilde{\beta}}_i(t) - v_i^2(t)e_{v,i}(t)) + \\ & \tilde{\delta}_i(t)(\dot{\tilde{\delta}}_i(t) - e_{v,i}(t)) + \bar{\alpha}_i(\dot{\tilde{\bar{\alpha}}} + \tau_i(t)e_{v,i}(t)) \\ =& - k_1 e_{v,i}^2(t) \leq 0 \end{aligned} \tag{17}$$

which implies that $e_{v,i}$ is bounded and square-integrable, which in turn implies that all the other signals in the closed-loop system are bounded. Hence, further by (12), $\dot{e}_{v,i}$ is bounded. Therefore, applying Barbalat's lemma (Ioannou and Fidan (2006)), we conclude that $\lim_{t\to\infty} e_{v,i}(t) = 0$ for $k_1, k_2 > 0$. This completes the proof. □

4.2 Lateral controller

The objective of the lateral controller is to keep the vehicle on the reference path, maintain the lateral spacing between neighbours and follow the curved road, all by controlling the front steering angle ϕ_i. To achieve this goal, we use the following (inverse kinematic) lateral controller proposed in Linderoth et al. (2008) which aims to bring the yaw angle error e_ψ and lateral displacement error e_l to zero under the assumption that each vehicle moves forward ($v_i(t) > 0$):

$$\tan(\phi_i) = \frac{-\cos\left(e_{\psi,i}\right)e_l - (k_{a,1} + k_{a,2})\sin\left(e_{\psi,i}\right)}{k_{a,1} - (k_{a,1} + k_{a,2})\cos\left(e_{\psi,i}\right) + \sin\left(e_{\psi,i}\right)e_{l,i}} \tag{18}$$

where $k_{a,1}, k_{a,2}$ are coefficients greater than zero. Since both the vehicle position and reference are expressed in the Frenet coordinates, the vehicle orientation is equal to the heading error $e_{\psi,i}(t) = -\psi_i(t)$ while the lateral error is defined as $e_{l,i}(t) = l_{lane} - l_{i,des}(t) - l_i(t)$, where l_{lane} is the l coordinate of the lane to which the vehicle belongs.

4.3 Distributed formation control scheme

In Hendrickx et al. (2019), the authors apply a switching control scheme that ensures that the inter-agent distances remain bounded in the presence of bounded sensor noise. They propose to apply non-linear threshold functions

$$T_w(x) = \begin{cases} x & \text{if } |x| > w \\ 0 & \text{otherwise.} \end{cases} \tag{19}$$

for robustness against the effects of the distance measurement disturbances $n_{ij}(t)$. However, any non-decreasing function for which $T_w(x) = 0$ only if $|x| \leq w$ can be applied. This design ensures that the agent only moves when there is no doubt that it moves in the right direction. The framework in Hendrickx et al. (2019) is defined for 1-dimensional platoon formations and we observe that in (7), each dimension is addressed independently of the others. Therefore, we can apply the threshold function to both the longitudinal and lateral direction and obtain the same convergence guarantees.

Thus, considering only the longitudinal direction, we express the formation control algorithm robust to noise as

$$\begin{aligned} u_{i,s}(t) = \; & k_s T_{deg(i)\bar{n}}\Big(\sum_{j\in\mathcal{N}_i} w_{ji}(t)(s_j(t) - s_i(t) \\ & + n_{ji}(t) - D_{ji})\Big) + v_f \end{aligned} \tag{20}$$

where $k_s > 0$ is the control gain, v_f is the desired forward group speed and $deg(i)$ is the degree of the vehicle in the graph G. Furthermore, a saturation function ensures that the vehicles adhere to minimum and maximum speeds and $T_{deg(i)\bar{n}}$ is defined as

$$T_{\bar{n}}(x) = \begin{cases} x & \text{if } |x| > \bar{n} + k_n \\ 0 & \text{if } |x| \leq \bar{n} \\ \dfrac{(|x| - \bar{n})\,\mathrm{sgn}(x)}{k_n}|x| & \text{else} \end{cases} \tag{21}$$

where $k_n > 0$ is a design constant. The controller for the lateral direction is defined as

$$u_{i,l}(t) = k_l T_{deg(i)\bar{n}}\Big(\sum_{j\in\mathcal{N}_i} w_{ji}(t)(l_j(t) - l_i(t) + n_{ji}(t) - D_{ji})\Big) \tag{22}$$

where $k_l > 0$ is the control gain.

Now we consider N vehicles with positions $s_1(t), \ldots, s_N(t) \in \mathbb{R}$ and $l_1(t), \ldots, l_N(t) \in \mathbb{R}$ at time instant t and a connected undirected sensing graph G. Under the control laws (20), (21) and (22), for any realizable desired relative positions D_{ij}, by the framework in Hendrickx et al. (2019) it is then guaranteed that:

Table 1. System and control parameters

Parameter	Value	Parameter	Value
k_s	0.6	k_1	7
k_l	0.1	k_2	1
$k_{a,1}$	1	v_{min}, v_{max}	10, 40 [m/s]
$k_{a,2}$	2	v_f	25 [m/s]
k_n	0.06	$\bar{n}$	0.4 [m]

- $\bar{s} = \lim_{t\to\infty} s(t)$ exists, and satisfies
$$\left| \sum_{j\in\mathcal{N}_i} (\bar{s}_j - \bar{s}_i - D_{ji}) \right| \leq 2deg(i)\bar{n} \tag{23}$$
where $\bar{n}$ is the bound on the disturbance.
- For every agent i and for all $t \in \mathbb{R}_{\geq 0}$ it holds
$$s_i^*(t) + \min_j(s_j(t) - s_j^*(t)) \leq s_i(t) \leq s_i^*(t) + \max_j \left(s_j(t) - s_j^*(t)\right) \tag{24}$$
where $s^*(t) \in \mathbb{R}^N$ is a realization D_{ij}, i.e., $D_{ij} = s_i^*(t) - s_j^*(t),\ (i,j) \in \mathcal{E}$

The vehicles are thus guaranteed to reach the region defined by the threshold function but they will regulate (5) to a vicinity of zero instead of exactly zero. It is important to note that this formulation only considers the effect of sensor noise while neglecting the effects of, among others, the performance of the lower-level control loop and a certain elasticity of the formation. The region defined for the threshold function can be extended to encompass these effects as well but the analysis of this extension is considered a future research direction.

Controller weights: Each vehicle aims to maintain the desired relative position to all its neighbours, meaning vehicles in both its own and adjacent lanes. However, there is no distinction between lanes even though proximity to a vehicle in the same lane would sooner result in a collision. To address this, vehicles should prioritize the distance with others in the same lane which can be achieved by redefining the weights. In longitudinal control, vehicles that are in the same lane will receive a higher weight than those in other lanes. To ensure that the redistribution of priorities never introduces an error larger than defined by the threshold function, the weights are required to satisfy

$$\sum_{j\in\mathcal{N}_i} (w_{ji}(t) n_{ji}(t)) \leq deg(i)\bar{n} \tag{25}$$

Then the weights for the longitudinal and lateral directions are respectively computed as:

$$w_{ji,s}(t) = \frac{deg(i)(\sum_{j\in\mathcal{N}_i}(|d_{ji,l}(t)|) - |d_{ji,l}(t)|)}{(deg(i)-1)\sum_{j\in\mathcal{N}_i}(|d_{ji,l}(t)|)} \tag{26}$$

$$w_{ji,l}(t) = \frac{deg(i)(\sum_{j\in\mathcal{N}_i}(|d_{ji,s}(t)|) - |d_{ji,s}(t)|)}{(deg(i)-1)\sum_{j\in\mathcal{N}_i}(|d_{ji,s}(t)|)} \tag{27}$$

5. SIMULATIONS

This section presents the results of an example simulation among the many numerical simulations performed to validate the proposed control framework. Consider five vehicles for which the underlying graph capturing the interaction between vehicles is illustrated in Fig. 4. The simulation employs control laws (10), (18), (20) and (22).

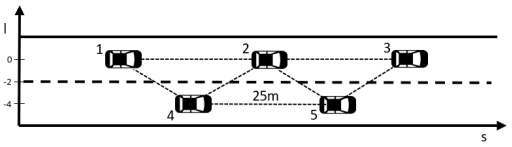

Fig. 4. A formation of five vehicles in Frenet coordinates

The initial positions and speeds of the vehicles are set as $p_1(0) = [0, -0.3]^T$, $p_2(0) = [22, 0]^T$, $p_3(0) = [48, 0.5]^T$, $p_4(0) = [10, -3.4]^T$, $p_5(0) = [45, -4]^T$ [m] and $v_1(0) = 30$, $v_2(0) = 25$, $v_3(0) = 26$, $v_4(0) = 31$, $v_5(0) = 27$ [m/s] respectively. The values of the assumed system and control parameters are given in Table 1 and the unknown parameters for the longitudinal dynamics of the vehicles are assumed to be $\alpha = [\alpha_1, \alpha_2, \alpha_3, \alpha_4, \alpha_5]^T = [1.2, 1, 2.5, 2, 1.4]^T 10^{-3}$, $\beta = [\beta_1, \beta_2, \beta_3, \beta_4, \beta_5]^T = [-1, -1, -1.1, -0.9, -1.1]^T 10^{-4}$, $\delta = [\delta_1, \delta_2, \delta_3, \delta_4, \delta_5]^T = [-0.1, -0.12, -0.09, -0.1, -0.098]^T$. We consider the platoon to be driving on a curved road with a constant curve radius of 175 [m]. For the sensor disturbances $n_{ij}(t)$, we apply pulse signals as in Hendrickx et al. (2019). Fig. 5 shows that the error between the planned and actual velocity tends to zero as expected from Theorem 1. Fig. 6 shows the errors in the desired inter-vehicle longitudinal distances as the platoon moves to achieve its control objectives. The results indicate a minor effect of the pulse signal while the agents converge but it diminishes once they stabilize on the interval defined by (23). The errors in inter-vehicle distances in the same lane tend to the threshold interval faster than those in different lanes, demonstrating the controller weight prioritization.

The defined threshold intervals have a size of only 2%-4% of the magnitudes of the desired relative positions, which we consider to be well within a safe margin. It should be noted that, even though we can define a specific $\bar{n}$ for each dimension, this region then holds for all desired relative positions in that dimension independent of their size. There is, unfortunately, no way around this, as applying the thresholds to measurements as opposed to control actions, does not guarantee that vehicles would converge to the desired interval (Hendrickx et al. (2019)).

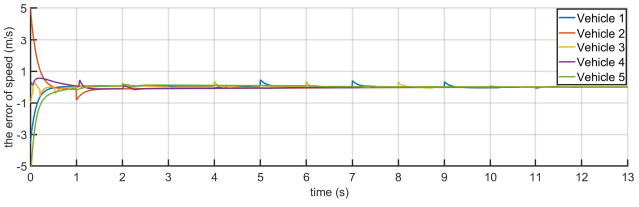

Fig. 5. Longitudinal speed tracking error for five agents

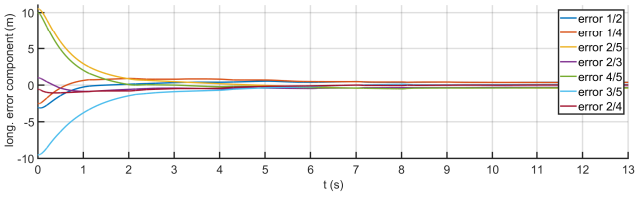

Fig. 6. Evolution with time of the longitudinal component of the errors $e_{ij} = p_i - p_j - D_{ij}$ for a five agent platoon

6. CONCLUSION AND FUTURE WORK

In this paper, we designed a novel distributed formation control and coordination scheme for multi-lane heterogeneous vehicle platoons with a bi-level framework consisting of formation and dynamic control layers. Frenet coordinates are utilized in the design of the formation control scheme to allow the platoon to adapt to the shape of the road. The proposed distributed formation control scheme is relative position based and aims to achieve a desired geometric formation and common group velocity in the presence of bounded sensor noise in the inter-agent relative position measurements. Adaptive longitudinal controllers enable the platoon of heterogeneous vehicles to track the desired platoon velocity and lateral controllers adjust the steering angle to keep them to the lane and formation. The conflicting nature of the control objectives and uncertainty in the system required a solution within margins rather than an exact one. This suits a platooning application well as the control needs to be more conservative to prioritize robustness over achieving an optimal configuration.

One future research topic is an extension of the threshold function properties analysis with desired relative position intervals. Another follow-up topic is analysing the effect of, among others, the performance of the lower-level control loop and a certain elasticity of the formation in the deadzone. Finally, this paper assumed a static formation and group velocity, but it would be beneficial to investigate dynamic adjustments based on desired platoon movements.

REFERENCES

Buzeman, D., Viano, D., and Lövsund, P. (1998). Car occupant safety in frontal crashes: a parameter study of vehicle mass, impact speed, and inherent vehicle protection. *Accident Analysis & Prevention*, 30(6), 713–722.

Cai, M., Xu, Q., Li, K., and Wang, J. (2019). Multi-lane formation assignment and control for connected vehicles. In *2019 IEEE Intelligent Vehicles Symposium (IV)*, 1968–1973. IEEE.

Chan, E., Gilhead, P., Jelinek, P., Krejci, P., and Robinson, T. (2012). Cooperative control of sartre automated platoon vehicles. In *19th ITS World CongressERTICO-ITS EuropeEuropean Commission-ITS AmericaITS Asia-Pacific*.

Cudrano, P., Mentasti, S., Matteucci, M., Bersani, M., Arrigoni, S., and Cheli, F. (2020). Advances in centerline estimation for autonomous lateral control. In *2020 IEEE Intelligent Vehicles Symposium (IV)*, 1415–1422. IEEE.

De La Fortelle, A., Qian, X., Diemer, S., Grégoire, J., Moutarde, ., Bonnabel, S., Marjovi, A., Martinoli, A., Llatser, I., Festag, A., et al. (2014). Network of automated vehicles: the autonet2030 vision. In *21st World Congress on Intelligent Transport Systems*.

De Marina, H., Cao, M., and Jayawardhana, B. (2014). Controlling rigid formations of mobile agents under inconsistent measurements. *IEEE Transactions on Robotics*, 31(1), 31–39.

Dolk, V., Ploeg, J., and Heemels, W. (2017). Event-triggered control for string-stable vehicle platooning. *IEEE Transactions on Intelligent Transportation Systems*, 18(12), 3486–3500.

Firoozi, R., Zhang, X., and Borrelli, F. (2021). Formation and reconfiguration of tight multi-lane platoons. *Control Engineering Practice*, 108, 104714.

Guanetti, J., Kim, Y., and Borrelli, F. (2018). Control of connected and automated vehicles: State of the art and future challenges. *Annual reviews in control*, 45, 18–40.

Hendrickx, J., Gerencsér, B., and Fidan, B. (2019). Trajectory convergence from coordinate-wise decrease of quadratic energy functions, and applications to platoons. *IEEE Control Systems Letters*, 4(1), 151–156.

Huang, M. and Manton, J. (2009). Coordination and consensus of networked agents with noisy measurements: Stochastic algorithms and asymptotic behavior. *SIAM Journal on Control and Optimization*, 48(1), 134–161.

Ioannou, P. and Fidan, B. (2006). *Adaptive control tutorial*. SIAM.

Kato, S., Tsugawa, S., Tokuda, K., Matsui, T., and Fujii, H. (2002). Vehicle control algorithms for cooperative driving with automated vehicles and intervehicle communications. *IEEE Transactions on intelligent transportation systems*, 3(3), 155–161.

Li, S., Gao, F., Li, K., Wang, L., You, K., and Cao, D. (2017a). Robust longitudinal control of multi-vehicle systems—a distributed h-infinity method. *IEEE Transactions on Intelligent Transportation Systems*, 19(9), 2779–2788.

Li, S., Zheng, Y., Li, K., Wu, Y., Hedrick, J., Gao, F., and Zhang, H. (2017b). Dynamical modeling and distributed control of connected and automated vehicles: Challenges and opportunities. *IEEE Intelligent Transportation Systems Magazine*, 9(3), 46–58.

Li, Y., Tang, C., Peeta, S., and Wang, Y. (2018). Integral-sliding-mode braking control for a connected vehicle platoon: Theory and application. *IEEE Transactions on Industrial Electronics*, 66(6), 4618–4628.

Linderoth, M., Soltesz, K., and Murray, R. (2008). Nonlinear lateral control strategy for nonholonomic vehicles. In *2008 American control conference*, 3219–3224. IEEE.

Navarro, I., Zimmermann, F., Vasic, M., and Martinoli, A. (2016). Distributed graph-based control of convoys of heterogeneous vehicles using curvilinear road coordinates. In *2016 IEEE 19th International Conference on Intelligent Transportation Systems (ITSC)*, 879–886.

Oh, K., Park, M., and Ahn, H. (2015). A survey of multi-agent formation control. *Automatica*, 53, 424–440.

Ren, W., Beard, R., and McLain, T. (2005). Coordination variables and consensus building in multiple vehicle systems. In *Cooperative control*, 171–188. Springer.

Sancar, F., Fidan, B., and Huissoon, J. (2015). Deadzone switching based cooperative adaptive cruise control with rear-end collision check. In *2015 International Conference on Advanced Robotics (ICAR)*, 283–287. IEEE.

Smith, M. (2016). The number of cars worldwide is set to double by 2040. In *World Economic Forum, Geneva*.

Yeong, D., Velasco-Hernandez, G., Barry, J., Walsh, J., et al. (2021). Sensor and sensor fusion technology in autonomous vehicles: A review. *Sensors*, 21(6), 2140.

Zheng, Y., Wang, Q., Cao, D., Fidan, B., and Sun, C. (2021). Distance-based formation control for multi-lane autonomous vehicle platoons. *IET Control Theory & Applications*, 15(11), 1506–1517.